BFKL Pomeron in (2+1)-dimensional QCD

D. Yu. Ivanov,[1,2] R. Kirschner,[1] E. M. Levin,[3,4] L. N. Lipatov,[4] L. Szymanowski,[1,5] and M. Wüsthoff[6]
[1]*Naturwissenschaftlich-Theoretisches Zentrum and Institut für Theoretische Physik, Universität Leipzig, Augustusplatz 10, D-04109 Leipzig, Germany*
[2]*Institute of Mathematics, 630090 Novosibirsk, Russia*
[3]*School of Physics and Astronomy, Tel Aviv University, Ramat Aviv, 69978 Israel*
[4]*St. Petersburg Nuclear Physics Institute, 188350 Gatchina, St. Petersburg, Russia*
[5]*Soltan Institute for Nuclear Studies, Hoża 69, 00-681 Warsaw, Poland*
[6]*University of Durham, Department of Physics, South Road, Durham City DH1 3LE, United Kingdom*
(Received 30 April 1998; published 9 September 1998)

We investigate high-energy scattering in spontaneously broken Yang-Mills gauge theory in $2+1$ space-time dimensions and present the exact solution of the leading $\ln s$ BFKL equation. The solution is constructed in terms of special functions using the earlier results of two of us (L.N.L. and L.S.). The analytic properties of the t-channel partial wave as functions of the angular momentum and momentum transfer have been studied. We find in the angular momentum plane (i) a Regge pole whose trajectory has an intercept larger than 1 and (ii) a fixed cut with the rightmost singularity located at $j=1$. The massive Yang-Mills theory can be considered as a theoretical model for the (nonperturbative) Pomeron. We study the main structure and property of the solution including the Pomeron trajectory at momentum transfer different from zero. The relation to the results of Li and Tan for the massless case is discussed. [S0556-2821(98)03119-1]

PACS number(s): 12.38.Bx, 11.15.Ex

I. INTRODUCTION

Recent experimental data from the DESY *ep* collider HERA [1] on deep inelastic scattering at small x and fixed Q^2 and from the Fermilab Tevatron on high-energy diffraction [2] revived interest in the long standing problem of the Pomeron structure and of the relation between soft and hard processes at high energy.

For the hard Regge processes one can use the Balitskii-Fadin-Kuraev-Lipatov (BFKL) theory [3], but we are lacking a self-consistent theoretical approach to the soft Pomeron and have to rely merely on general properties of analyticity, causality, and crossing symmetry in developing an extended and successful phenomenology of high-energy soft interactions [4,5,6].

Some theoretical understanding of the Pomeron has been derived from the study of the leading $\ln s$ approximation of superrenormalizable models such as $\lambda\phi^3$ in $3+1$ dimensions. The main features of the result have been included in the parton model of peripheral interactions and they are the basis of our understanding of the Pomeron structure [7,8]. However, such models result in Regge singularities with an intercept of around -1 and do not reproduce essential features of the Pomeron. Much effort has been applied to show the self-consistency of the Pomeron hypothesis in the framework of Reggeon field theory or Gribov's Reggeon calculus [9]. A Reggeon field theory approach to QCD has been developed in [10].

On the contrary, for the hard Pomeron we can apply perturbative QCD and derive a number of detailed predictions [11]. The BFKL Pomeron [3] appearing in the leading $\ln s$ [$\approx \ln(1/x)$] approximation plays a special role. The main features of the BFKL Pomeron, however, look different from properties of the soft Pomeron.

In this paper we study the BFKL Pomeron in spontaneously broken $(2+1)$-dimensional gauge theory, using previous results obtained in Ref. [12]. One can consider this theory as a simple model for the soft Pomeron. Indeed we show that the resulting BFKL Pomeron is a normal moving Regge pole with its intercept $\alpha_P(0)>1$.

The coupling of this theory has the dimension of mass. The interaction is superrenormalizable. This results in the absence of scaling violations of structure functions due to ultraviolet divergences. On the other hand, the infrared singularities in the massless limit are stronger compared to $(3+1)$-dimensional QCD. The comparison allows us to discuss the influence of the ultraviolet and infrared singularities on the Pomeron structure.

In QCD (massless gluons in $3+1$ dimensions) the known way [13] of solving the BFKL equation relies on conformal symmetry. This approach is useless in the case of massive gauge bosons. Up to now the solution has not been known for the massive case. In the special case of $2+1$ dimensions, however, the equation exhibits a simple iterative structure which allows one to construct a solution. The experience gained in the $(2+1)$-dimensional theory will be helpful in solving the corresponding equation in the physical case.

We obtain the exact solution both for the forward and nonforward cases, and calculate the partial wave amplitude for the scattering of two massive gauge bosons. We investigate the Regge singularities in the complex angular momentum plane and their behavior in dependence of the momentum transfer.

The paper is based on an early investigation by two of the authors [12], where the basic idea of the iterative solution was formulated for the general nonforward case. This investigation was motivated in particular by [15], where the BFKL equation with the infrared regularization has been considered. We discuss the relation of our result with the one by Li and Tan [14] where the massless $(2+1)$-dimensional gauge theory has been considered.

II. BFKL EQUATION WITH MASSIVE GLUONS

A. 3+1 dimensions

Let us start with a short reminder of the results obtained within the leading logarithmic approximation (LLA) of perturbation theory for the amplitudes of the high-energy scattering in the spontaneously broken Yang-Mills theory [3]. We discuss the simplest case of the SU(2) gauge group with symmetry breaking by one Higgs doublet (fundamental representation). This is the case discussed in [3]; we shall follow the notation of that paper. The generalization to the SU(N) gauge group is straightforward and is done in Sec. III C. Notice that the details depend on the type of symmetry breaking. We consider the case that all gauge bosons become massive.

The amplitude describing the elastic two-particle scattering $AB \to A'B'$ can be decomposed into the amplitudes with definite isotopic spin T in the t channel, with $T=0,1,2$:

$$A_{AB}^{A'B'} = \Gamma_{AA'} A^{(0)} \Gamma_{BB'} + \Gamma^i_{AA'} A^{(1)} \Gamma^i_{BB'} + \Gamma^{ij}_{AA'} A^{(2)} \Gamma^{ij}_{BB'}. \tag{2.1}$$

The constants Γ in Eq. (2.1) depend on the kind of scattering particles (gauge bosons, fermions, Higgs particles), and they are all proportional to the coupling constant $\Gamma \propto g$; for their explicit forms see [3].

In what follows we shall concentrate on the singlet part of the amplitude (2.1). $A^{(0)}$ is related to the partial wave $F_\omega(q^2)$ in the following way ($j=1+\omega$):

$$A^{(0)}(s,q) = \frac{s}{4i} \int_{\delta - i\infty}^{\delta + i\infty} d\omega \left(\frac{s}{m^2} \right)^{\omega} \frac{e^{-i\pi\omega}-1}{\sin \pi\omega} F_\omega(q^2),$$

$$t=-q^2, \tag{2.2}$$

$$F_\omega(q^2) = \frac{1}{\omega} \frac{g^2}{(2\pi)^3} \int \frac{d^2k}{(k^2+m^2)[(k-q)^2+m^2]} \times f_\omega(k,q-k) A_0(q^2), \tag{2.3}$$

$$A_0(q^2) = -2\left(q^2 + \frac{5}{4} m^2 \right). \tag{2.4}$$

We write here and in the following the scalar products of transverse momenta in Euclidean notation. The function $f_\omega(k,q-k)$ satisfies the following integral equation (see Fig. 1 for notation and a graphic form of the equation):

$$[\omega - \alpha(k^2) - \alpha((k-q)^2)] f_\omega(k,q-k) = \frac{\omega}{A(q^2)} + \frac{g^2}{(2\pi)^3} \int \frac{d^2k_1}{(k_1^2+m^2)[(k_1-q)^2+m^2]} \times K(k,k_1,q) f_\omega(k_1,q-k_1), \tag{2.5}$$

with the kernel

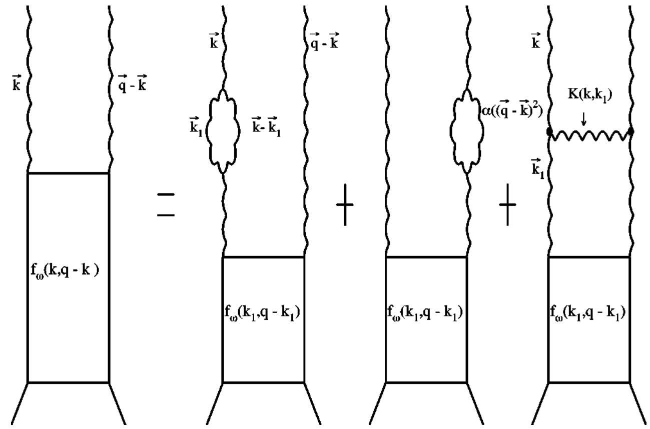

FIG. 1. The graphic form of the BFKL equation.

$$K(k,k_1,q) = A_0(q^2) + \frac{2}{(k-k_1)^2+m^2} \times \{(k^2+m^2)[(k_1-q)^2+m^2] + (k_1^2+m^2)[(k-q)^2+m^2]\} \tag{2.6}$$

and the Regge trajectory of the massive gluons:

$$\alpha(k^2) = j-1 = -\frac{g^2(k^2+m^2)}{(2\pi)^3} \int \frac{d^2k_1}{(k_1^2+m^2)[(k_1-k)^2+m^2]}. \tag{2.7}$$

As a consequence of the integral equation (2.5) it is possible to express the partial wave $F_\omega(q^2)$ through the solution of Eq. (2.5) on the mass shell:

$$f_\omega(k,k-q)|_{k^2=(q-k)^2=-m^2} = F_\omega(q^2) + A_0^{-1}(q^2). \tag{2.8}$$

B. 2+1 dimensions

In Refs. [12,15] it was established that in $(2+1)$-dimensional space-time the high-energy scattering amplitudes derived in the LLA are given by formulas similar to the ones from the previous section. The main difference is that the transverse space in this case is one dimensional, and so the substitution

$$\frac{d^2k}{(2\pi)^2} \to \frac{dk}{2\pi}$$

should be made.

Therefore

$$F_\omega(q^2) = \frac{1}{\omega} \frac{g^2}{(2\pi)^2} \int \frac{dk}{(k^2+m^2)[(k-q)^2+m^2]} \times f_\omega(k,q-k) A_0(q^2), \tag{2.9}$$

where now g^2 carries the dimension of mass.

The Regge trajectory for massive vector bosons in the $2+1$ dimensions is given by the simple rational expression

$$\alpha(k^2)=-\frac{g^2(k^2+m^2)}{(2\pi)^2}\int\frac{dk_1}{(k_1^2+m^2)[(k_1-k)^2+m^2]}$$
$$=-\frac{g^2}{2\pi m}\frac{k^2+m^2}{k^2+4m^2}. \tag{2.10}$$

For the function $f_\omega(k,q-k)$ we have here the one-dimensional Bethe-Salpeter-type equation

$$[\omega-\alpha(k^2)-\alpha((k-q)^2)]f_\omega(k,q-k)$$
$$=\frac{\omega}{A(q^2)}+\frac{g^2}{(2\pi)^2}\int\frac{dk_1}{(k_1^2+m^2)[(k_1-q)^2+m^2]}$$
$$\times K(k,k_1,q)f_\omega(k_1,q-k_1). \tag{2.11}$$

Our aim is to find the analytic solution of this equation. It is convenient to introduce the dimensionless variables

$$\alpha_S=\frac{g^2}{4\pi m},\quad \epsilon=\frac{g^2}{2\pi m\omega}=\frac{2\alpha_S}{\omega},\quad k\to mk,\quad q\to mq. \tag{2.12}$$

Then Eq. (2.11) takes the form

$$\left[1+\epsilon\left(\frac{k^2+1}{k^2+4}+\frac{(k-q)^2+1}{(k-q)^2+4}\right)\right]f_\omega(k,q-k)$$
$$=A_0^{-1}+\epsilon\int\frac{dk_1}{2\pi}\left(\frac{A_0}{(k_1^2+1)[(k_1-q)^2+1]}+\frac{2}{(k-k_1)^2+1}\right.$$
$$\left.\times\left[\frac{k^2+1}{k_1^2+1}+\frac{(k-q)^2+1}{(k_1-q)^2+1}\right]\right)f_\omega(k_1,q-k_1), \tag{2.13}$$

$$A_0=-(2q^2+\tfrac{5}{2}). \tag{2.14}$$

The remaining equations of the previous section are unchanged.

In order to present the main steps of our method for finding the exact solution of Eq. (2.13) we consider first the simpler case with vanishing momentum transfer $q=0$.

III. FORWARD SCATTERING AT HIGH ENERGY

In the case with vanishing momentum transfer $q=0$, Eq. (2.13) takes the simpler form

$$\frac{(1+2\epsilon)(k^2+\lambda^2)}{k^2+4}f_\omega(k)-A_0^{-1}$$
$$=\epsilon\int\frac{dk_1}{2\pi}\left(\frac{A_0}{(k_1^2+1)^2}+\frac{4}{(k-k_1)^2+1}\frac{k^2+1}{k_1^2+1}\right)f_\omega(k_1), \tag{3.1}$$

where we have introduced the convenient notation

$$\lambda^2=\frac{4+2\epsilon}{1+2\epsilon}. \tag{3.2}$$

In this case we present the methods of solution both in coordinate and momentum representations. In this way different aspects of the problem will be illuminated.

A. Coordinate space analysis

We find that it is convenient to work with the function $\phi_\omega(k)=(k^2+1)^{-1}f_\omega(k)$. Equation (3.1) is a linear inhomogeneous integral equation. We try to solve it in coordinate space by introducing

$$\phi_\omega(k)=\int dx\, e^{ikx}\phi_\omega(x). \tag{3.3}$$

The main advantage of the coordinate space is the fact that the BFKL kernel in Eq. (3.1) looks simple due to the relation

$$\int\frac{dk}{2\pi}\frac{e^{ikx}}{k^2+1}=\frac{1}{2}e^{-|x|}. \tag{3.4}$$

Substituting Eq. (3.3) and Eq. (3.4) in Eq. (3.1) we obtain

$$(1+2\varepsilon)\left(-\frac{d^2}{d^2x}+\lambda^2\right)\phi_\omega(x)$$
$$=\frac{1}{2A_0}[3e^{-|x|}+2\delta(x)]+2\varepsilon\left(-\frac{d^2}{d^2x}+4\right)e^{-|x|}\phi_\omega(x)$$
$$-\frac{\varepsilon A_0}{4}[3e^{-|x|}+2\delta(x)]\int dy\,\phi_\omega(y)e^{-|y|}, \tag{3.5}$$

where $\delta(x)$ is the Euler δ function. We shall analyze Eq. (3.5) without the inhomogeneous term in order to investigate the leading eigenvalue ε.

$\phi_\omega(x)$ should be bound for the Fourier transform (3.3) to exist. At large $|x|$ only the left-hand side of Eq. (3.5) is important which leads to the asymptotic solution $e^{-\lambda|x|}$.

Clearly the solution depends on $|x|$ only because the kernel $K(x)$ is an even function of x. We introduce a new function

$$\Phi_\omega(x)=[1+2\varepsilon(1-e^{-|x|})]\phi_\omega(x) \tag{3.6}$$

and a new variable $z=e^{-|x|}$.

For the function Φ_ω the equation looks as follows:

$$-z\frac{d}{dz}z\frac{d\Phi_\omega(z)}{dz}+2z\frac{d\Phi_\omega(z)}{dz}\delta(z-1)+4\Phi_\omega(z)$$
$$=6\varepsilon\frac{\Phi_\omega(z)}{1+2\varepsilon(1-z)}+\frac{A_0\varepsilon}{4}[3z+2\delta(z-1)]$$
$$\times\int_0^1 dz'\frac{\Phi_\omega(z')}{1+2\varepsilon(1-z')}. \tag{3.7}$$

Comparing the coefficients in front of the δ functions we obtain

$$\left.\frac{d\Phi_\omega(z)}{dz}\right|_{z=1}=\frac{\epsilon A_0}{4}\int_0^1 dz'\frac{\Phi_\omega(z')}{1+2\varepsilon(1-z')}, \tag{3.8}$$

which will give the equation for the position of the pole in the angular momentum plane (the intercept of the Pomeron) as will be shown below. The second condition

$$\Phi_\omega(z)\to 0 \quad at \quad z\to 0 \tag{3.9}$$

follows from the large $|x|$ behavior of $\phi_\omega(x)$ discussed above.

The important observation is that a solution of Eq. (3.7) obeying Eq. (3.9) can be found in the form

$$\Phi_\omega(z)=Cz[1+2\varepsilon(1-z)]+\Phi_\omega^{hg}(z), \tag{3.10}$$

where $\Phi_\omega^{hg}(z)$ is the solution of the homogeneous equation

$$-z\frac{d}{dz}z\frac{d\Phi_\omega^{hg}(z)}{dz}+4\Phi_\omega^{hg}(z)=6\varepsilon\,\frac{\Phi_\omega^{hg}(z)}{1+2\varepsilon(1-z)}, \tag{3.11}$$

and C is a constant in z, which, however, depends on the function Φ_ω:

$$C=-\frac{5\varepsilon}{8+\frac{5}{2}\varepsilon}\int_0^1 dz'\,\frac{\Phi_\omega^{hg}}{1+2\varepsilon(1-z')}. \tag{3.12}$$

The solution of the homogeneous equation (3.11) can be easily found. We obtain

$$\Phi_\omega^{hg}(z)=Nz^\lambda{}_2F_1\left(2+\lambda,-2+\lambda,1+2\lambda,\frac{2\varepsilon z}{1+2\varepsilon}\right)$$
$$=N\frac{[1+2\varepsilon(1-z)]z^\lambda}{1+2\varepsilon}\times{}_2F_1\left(3+\lambda,-1+\lambda,1+2\lambda,\frac{2\varepsilon z}{1+2\varepsilon}\right). \tag{3.13}$$

Here ${}_2F_1$ is the Gauss hypergeometric function and the constant N can be defined from the normalization.

To find the value of ε which corresponds to the bound state we have to solve Eq. (3.8) which using well-known properties of the hypergeometric function can be reduced to the form

$$\frac{5-2\lambda^2}{4-\lambda^2}\,{}_2F_1\left(3+\lambda,-1+\lambda,1+2\lambda,\frac{4-\lambda^2}{3}\right)+\frac{(\lambda^2-1)(\lambda-1)}{\lambda^2-4}\,{}_2F_1\left(3+\lambda,\lambda,1+2\lambda,\frac{4-\lambda^2}{3}\right)$$
$$=\frac{2}{1+\frac{16}{5}[(1-\lambda^2)/(\lambda^2-4)]}\frac{1}{2+\lambda}\left[{}_2F_1\left(2+\lambda,-1+\lambda,1+2\lambda,\frac{4-\lambda^2}{3}\right)+\frac{1}{1+\lambda}\,{}_2F_1\left(1+\lambda,-1+\lambda,1+2\lambda,\frac{4-\lambda^2}{3}\right)\right]. \tag{3.14}$$

We solved this equation numerically and obtained the value $\varepsilon=\varepsilon_0=4.5934$ which leads to the rightmost singularity at $\omega=\omega_0=2\alpha_S/\varepsilon_0=0.436\alpha_S$ in accordance with Ref. [12].

The way we have solved the BFKL equation is reminiscent of the standard procedure of calculating bound states. The rightmost singularity in ω, a pole, corresponds to the ground state. In the following subsection we solve Eq. (3.1) in a momentum representation.

B. Momentum space analysis

We have to solve the linear inhomogeneous integral equation (3.1). It is possible to construct the solution directly by iterations. We rely on the relation

$$\int_{-\infty}^{\infty}\frac{dk'}{2\pi}\frac{1}{(k-k')^2+1}\frac{1}{k'^2+\lambda^2}=\frac{\lambda+1}{2\lambda[k^2+(\lambda+1)^2]}. \tag{3.15}$$

This means that the action of the kernel on $(k^2+\lambda^2)^{-1}$ can be expressed by the shift of the pole position $\lambda\to\lambda+1$.

Let us formally consider the right-hand side of Eq. (3.1) as a perturbation. We will consider first the solution of this equation in the interval $\epsilon\in[-1/2,\infty]$, where $\lambda^2>0$. We obtain the solution for $\lambda>0$ first and continue then analytically to the complete complex plane in ϵ or ω.

If we omit the right-hand side of Eq. (3.1) (the zeroth iteration), the solution is

$$f_\omega^{(0)}(k)=\frac{A_0^{-1}(k^2+4)}{(1+2\epsilon)(k^2+\lambda^2)}. \tag{3.16}$$

$f_\omega^{(0)}(k)$ can be represented as the sum of the constant term plus the pole term $\sim 1/(k^2+\lambda^2)$. In order to find the contribution arising from the next iteration ($f_\omega=f_\omega^{(0)}+f_\omega^{(1)}+\cdots$) let us substitute Eq. (3.16) into the right-hand side of Eq. (3.1). We use now Eq. (3.15) and obtain

$$\int_{-\infty}^{\infty}K(k,k_1,q=0)\frac{1}{k_1^2+\lambda^2}\frac{dk_1}{2\pi}$$
$$=\frac{A_0(\lambda+2)}{4\lambda(\lambda+1)^2}+\frac{2(k^2+1)}{\lambda(k^2+4)}\left[\frac{1}{\lambda+1}+\frac{\lambda+3}{k^2+(\lambda+1)^2}\right]. \tag{3.17}$$

We write the resulting first iteration $f_\omega^{(1)}$ as a sum of pole terms in k^2. In this expansion there are three terms: the constant term, the pole term $\sim 1/(k^2+\lambda^2)$, and as a new term, not encountered in the zeroth iteration $f_\omega^{(0)}$, the pole term $\sim 1/[k^2+(\lambda+1)^2]$. The same procedure can be applied to the subsequent iterations. It is easy to see that the expansion for the nth iteration will be given by the sum of the constant term plus the pole terms $A_k/(k^2+\lambda_k^2)$, $\lambda_k=\lambda+k-1$, $k=1,\ldots,n+1$. Therefore it is natural to look for the solution of Eq. (3.1) in the form [12]

$$f_\omega(k)=f_0+\sum_{n=1}^{\infty}\frac{A_n}{k^2+\lambda_n^2},\quad \lambda_n=\lambda+n-1. \tag{3.18}$$

Let us substitute this ansatz in Eq. (3.1). Comparing coefficients of the pole terms on both sides we find the condition

$$\frac{A_n}{A_{n-1}}=\frac{2\varepsilon}{1+2\varepsilon}\frac{(\lambda+n)(\lambda+n+1)}{(n-1)(2\lambda+n+1)}. \tag{3.19}$$

This recurrence relation has the following solution:

$$A_n=A_1\left(\frac{2\varepsilon}{1+2\varepsilon}\right)^{n-1}\frac{(\lambda_1+2)_{n-1}(\lambda_1+3)_{n-1}}{(n-1)!(2\lambda_1+1)_{n-1}}, \tag{3.20}$$

where $(a)_n=a(a+1)(a+2)\cdots(a+n-1)$. In this way we arrive at generalized hypergeometric functions ${}_{p+1}F_p\left({\alpha_1\cdots\alpha_{p+1} \atop \beta_1\cdots\beta_p}\middle|y\right)$ [16]. In particular, the ansatz (3.18) leads to

$$f_\omega(k)=f_0+\frac{A_1}{k^2+\lambda^2}\,{}_4F_3\left({\lambda_3,\lambda_4,\lambda+ik,\lambda-ik \atop 2\lambda+1,\lambda_2+ik,\lambda_2-ik}\middle|y\right), \tag{3.21}$$

with $\lambda_n=\lambda+n-1$, $\lambda=\lambda_1$, and $y=2\varepsilon/(1+2\varepsilon)$.

There are still two coefficients f_0 and A_1 undetermined in our solution (3.21). The information contained in Eq. (3.1) which has not been used yet can be expressed in terms of two conditions. The first condition appears as a result of the comparison of residua of the pole term $\sim 1/(k^2+\lambda^2)$ [the pole at $k^2\to\lambda^2$ has to be considered separately from other pole terms $\sim 1/(k^2+\lambda_n^2)$, $n\neq 1$]. The second condition appears as a result of the comparison of the constant terms appearing in the expansion or, in other words, considering the left- and right-hand sides of Eq. (3.1) at $k\to\infty$.

Therefore the coefficients f_0, A_1 are the solution of the following inhomogeneous system of linear equations:

$$-\frac{1}{A_0\epsilon}=f_0\cdot a_{11}+A_1\cdot a_{12},$$

$$-\frac{1}{A_0\epsilon}=f_0\cdot a_{21}+A_1\cdot a_{22}, \tag{3.22}$$

with

$$a_{11}=\frac{A_0}{4}+\frac{4(\lambda^2-1)}{(\lambda^2-4)},$$

$$a_{12}=-\frac{6}{(\lambda^2-4)^2}+\frac{A_0\lambda_3}{4\lambda\lambda_2^2}\,{}_4F_3\left({\lambda_4,\lambda_4,\lambda,\lambda_2 \atop 2\lambda+1,\lambda_3,\lambda_3}\middle|y\right)+\frac{4}{(\lambda^2-4)}\,{}_3F_2\left({\lambda_4,\lambda_2,\lambda-1 \atop 2\lambda+1,\lambda}\middle|y\right)+\frac{2\lambda_2}{\lambda(2\lambda+1)}\,{}_4F_3\left({\lambda_4,\lambda_3,\lambda-1,1 \atop 2\lambda+2,\lambda_2,2}\middle|y\right),$$

$$a_{21}=\frac{A_0}{4}+\frac{2(2\lambda^2-5)}{(\lambda^2-4)},$$

$$a_{22}=\frac{A_0\lambda_3}{4\lambda\lambda_2^2}\,{}_4F_3\left({\lambda_4,\lambda_4,\lambda,\lambda_2 \atop 2\lambda+1,\lambda_3,\lambda_3}\middle|y\right)+\frac{2}{\lambda\lambda_2}\,{}_2F_1\left({\lambda_4,\lambda \atop 2\lambda+1}\middle|y\right). \tag{3.23}$$

Using well-known relations among the hypergeometric functions [16] it is possible to express all higher hypergeometric functions through the two basic ${}_2F_1$ functions

$$f_a={}_2F_1\left({\lambda_2,\lambda \atop 2\lambda+1}\middle|y\right),$$

$$f_b={}_2F_1\left({\lambda,\lambda \atop 2\lambda+1}\middle|y\right). \tag{3.24}$$

We quote here only one of these relations:

$${}_4F_3\left({\lambda_4,\lambda_4,\lambda,\lambda_2 \atop 2\lambda+1,\lambda_3,\lambda_3}\middle|y\right)=f_a\frac{(7\lambda^2-4)}{(\lambda-1)\lambda_2\lambda_3^2}+f_b\frac{9\lambda^3}{(\lambda-1)^2\lambda_2^2\lambda_3^2}. \tag{3.25}$$

The solution of the system (3.1) expressed in terms of the functions f_a and f_b has the form

$$A_1=-\frac{\lambda_2^2\lambda_3^2(\lambda-2)}{A_0\epsilon}\left[\frac{A_0}{4}\left(f_a\frac{(13\lambda^2-16)}{\lambda}+18f_b\right)+f_a\frac{(34\lambda^2-64)(\lambda^2-1)}{\lambda(\lambda-2)\lambda_3}+f_b\frac{48\lambda^2-84}{(\lambda-2)\lambda_3}\right]^{-1},$$

$$f_0=\frac{3A_1}{(\lambda-1)(\lambda-2)\lambda_3^2\lambda_2^3}\left(f_a\lambda(1+2\lambda^2)+f_b\frac{3(\lambda^4+2)}{(\lambda-1)\lambda_2}\right). \tag{3.26}$$

These formulas together with Eq. (3.21) represent the solution of the integral equation (3.1).

It should be noted that in Ref. [12] instead of the first equation of the system (3.22) [resulting from the comparison of the residua of the pole terms $1/(k^2+\lambda^2)$ appearing on both sides of Eq. (3.1)] another boundary condition was used, the absence of the normal thresholds:

$$f_\omega(k^2\to -4)=2\,f_\omega(k^2\to -1). \tag{3.27}$$

This condition can be derived from Eq. (3.1) if one requires that $f_\omega(k)$ be a regular function in the neighborhood of $k^2=-4$. In terms of our ansatz this condition reads

$$f_0=A_1\left[\frac{1}{\lambda^2-4}\,{}_3F_2\left({}^{\lambda_3,\lambda_3,\lambda-2}_{2\lambda+1,\lambda-1}\middle|y\right)-\frac{2}{\lambda^2-1}\,{}_3F_2\left({}^{\lambda_4,\lambda_2,\lambda-1}_{2\lambda+1,\lambda}\middle|y\right)\right]. \tag{3.28}$$

The iterative solution of Eq. (3.1), $f_\omega(k)$, as described above, is a function which is by construction regular in the points $k^2=-n^2$. Therefore, the condition (3.28) should not give an additional restriction on the function (3.21) as compared with the conditions given by the system (3.22). Indeed, expressing the hypergeometric functions in Eq. (3.28) in terms of the functions f_a and f_b it can be checked directly that the difference of the two equations in Eqs. (3.22) and the condition (3.28) are equivalent.

C. Regge singularities of the forward partial wave

We discuss now the implications of the obtained solution $f_\omega(k)$ for the partial wave of the scattering amplitude F_ω. The partial wave F_ω can be calculated either by Eq. (2.9) or by the mass-shell relation (2.8). We have checked that both methods lead to the same result:

$$F_\omega(q=0)=\frac{-1}{A_0+f}, \tag{3.29}$$

where

$$f=\frac{4}{\lambda^2-4}\left(\frac{(34\lambda^2-64)(\lambda^2-1)}{\lambda}f_a+f_b(48\lambda^2-84)\right)\times\left(\frac{(13\lambda^2-16)}{\lambda}f_a+18f_b\right)^{-1}. \tag{3.30}$$

Let us discuss the singularities of F_ω considered as a function of the complex variable ω. The hypergeometric functions are defined in terms of the hypergeometric series which are convergent inside a circle of unit radius in the variable $y=2\epsilon/(1+2\epsilon)$. The continued hypergeometric functions are analytic in the complex plane of their argument y, with a cut from $y=1$ to $y=\infty$. In the ϵ plane this corresponds to the cut appearing on the interval $\epsilon\in[-\infty,-1/2]$.

As a function of their parameters $\alpha_1,\ldots,\alpha_{p+1}$, $\beta_1,\ldots,\beta_p$ the hypergeometric functions have only simple poles if one of the lower parameters $\beta_1,\ldots,\beta_p$ approaches a nonpositive integer value n. We see from Eqs. (3.2), (3.24) that both f_a and f_b have poles of this origin at $\lambda=\sqrt{(4+2\epsilon)/(1+2\epsilon)}\to-(1+n)/2$. Therefore these poles lie on the second (unphysical) sheet of the square root.

Further singularities of f_ω and, consequently, of F_ω appear at points, where the determinant of the system of linear equations (3.22) vanishes, i.e., at the zeros of the denominator in Eq. (3.29):

$$A_0+f=0. \tag{3.31}$$

This results in poles in ω.

Analyzing the condition (3.31) numerically outside the interval $\epsilon\in[-\infty,-1/2]$, where the cut is located, we have checked that there is only one Regge pole in the vicinity of the real axis located in

$$\epsilon=\epsilon_0=4.5934,\quad \omega=\omega_0=\frac{g^2}{2\pi m\epsilon_0}. \tag{3.32}$$

The result coincides of course with the one obtained in the coordinate representation. Therefore we can conclude that at $q=0$ the partial wave F_ω has the following singularities on the physical sheet of the complex ω plane. There is a finite cut on the negative part of the real axes covering the interval $\omega\in[\omega_2,\omega_1]$, with $\omega_2=-g^2/\pi m$, $\omega_1=0$. And there is a single pole in the positive part of the real axis at $\omega=\omega_0$, Eq. (3.32).

Let us discuss the nature of the singularities at the branch points. Near the right end point of the cut, $\omega=\omega_1=0$ we have $\epsilon\to+\infty$, $\lambda\to1$, $y\to1$, and

$$f_a=-2\left(1+\log\frac{2(\lambda-1)}{3}\right)+O((\lambda-1)\log(\lambda-1)),$$

$$f_b=2+O((\lambda-1)\log(\lambda-1)). \tag{3.33}$$

Therefore the partial wave behaves like

$$F_\omega\to-A_0^{-1}+16A_0^{-2}/\log(\lambda-1). \tag{3.34}$$

Near the left end point of the cut, $\omega=\omega_2$, we have $\epsilon\to-1/2$, $\lambda\to+\infty$, $y\sim-\lambda^2/3\to-\infty$, and

$$f_a=\frac{e^{\lambda(\log 12-2\log\lambda)}}{\sqrt{\pi\lambda}}[1+O(1/\lambda)], \tag{3.35}$$

$$f_b=\frac{e^{\lambda(\log 12-2\log\lambda)}\lambda\log\lambda}{\sqrt{\pi\lambda}}[1+O(1/\lambda)]. \tag{3.36}$$

Therefore the partial wave behaves like

$$F_\omega\to-\frac{1}{A_0+24/3}-\frac{1}{72(A_0+24/3)^2\log\lambda}. \tag{3.37}$$

Note that the solution of the corresponding homogeneous equation can be obtained from the solution of the inhomogeneous equation F_ω which we have just found. The spectrum consists of one discrete level $\omega=\omega_0$ and the continuous part $\omega\in[\omega_2,\omega_1]$. The corresponding eigenfunctions can be found as follows: the residue of F_ω of the pole at $\omega=\omega_0$ gives (up to the normalization constant) the wave function of the discrete level and by calculating the discontinuity of F_ω on the cut it is possible to find the eigenfunctions belonging to the continuous spectrum.

We would like to add a comment on how the results depend on the number of colors, N. In the case of arbitrary N we have to substitute, in the above equations [3],

$$g^2 \to g^2 \frac{N}{2}, \quad A_0 \to -2\left(q^2 + \frac{N^2+1}{N^2} m^2\right), \quad \epsilon \to \epsilon \frac{N}{2}. \tag{3.38}$$

As in the case $N=2$ there is a leading Regge pole at arbitrary N located at $\omega_0^{(N)}$:

$$\omega_0^{(N)} = \frac{g^2}{2\pi m} \frac{N}{2} \frac{1}{\epsilon_0^{(N)}}. \tag{3.39}$$

$\epsilon_0^{(N)}$ is calculated in analogy to ϵ_0 above. We find that $\epsilon_0^{(N)}$ decreases slowly with N approaching a limit $\epsilon_0^{(\infty)}$: $\epsilon_0^{(2)} = 4.5934$, $\epsilon_0^{(3)} = 3.8000$, $\epsilon_0^{(4)} = 3.5693$, $\epsilon_0^{(\infty)} = 3.3025$.

IV. NONFORWARD SCATTERING

A. Solution of the equation

The main steps which have been made in Sec. III B to derive the solution of the forward equation can be generalized to find the solution of the nonforward equation (2.13). The expression appearing on the left-hand side of Eq. (2.13) in the square brackets $[\cdots]$ can be rewritten in the form

$$[\cdots] = \frac{(1+2\epsilon)[x^2+(\lambda^+)^2][x^2+(\lambda^-)^2]}{[(x-q/2)^2+4][(x+q/2)^2+4]}, \tag{4.1}$$

where

$$x = k - q/2,$$

$$(\lambda^\pm)^2 = \frac{4+5\epsilon}{1+2\epsilon} - \frac{q^2}{4} \pm \sqrt{\frac{9\epsilon^2 - q^2(4+5\epsilon)(1+2\epsilon)}{(1+2\epsilon)^2}}. \tag{4.2}$$

Now, in analogy with the iterative way of finding the solution for $q=0$, we see that the zeroth iteration can be expanded into a sum of the constant term and two pole terms: $\sim 1/[x^2+(\lambda^+)^2]$ and $\sim 1/[x^2+(\lambda^-)^2]$. It should be noted that the zeroth iteration for $f_\omega(k,q-k)$ depends on the specific combination of the momenta k and $q-k$; i.e., it is a function of the variable $x^2=(k-q/2)^2$. The notation x should not be confused with the position. Calculating the next iterations it can be seen that this feature remains true and the solution can be represented in the following form [12]:

$$f_\omega(x^2) = f_0 + \sum_{n=1}^{\infty} \frac{A_n^+}{x^2+(\lambda_n^+)^2} + \sum_{n=1}^{\infty} \frac{A_n^-}{x^2+(\lambda_n^-)^2},$$

$$\lambda_n^\pm = \lambda^\pm + n - 1. \tag{4.3}$$

Substituting this ansatz into Eq. (2.13) we find two recurrence relations similar to the one for the case $q=0$. Their solutions can be written in the form

$$\frac{A_n^\pm}{A_1^\pm} = \left(\frac{2\epsilon}{1+2\epsilon}\right)^{n-1} \frac{1}{(n-1)!}$$
$$\times \frac{(\lambda_2^\pm)_{n-1}(\lambda_4^\pm + iq/2)_{n-1}(\lambda_4^\pm - iq/2)_{n-1}(\lambda^\pm - d_+^+)_{n-1}(\lambda^\pm - d_-^+)_{n-1}(\lambda^\pm - d_+^-)_{n-1}(\lambda^\pm - d_-^-)_{n-1}}{(\lambda^\pm)_{n-1}(2\lambda^\pm+1)_{n-1}(\lambda^\pm+\lambda^\mp+1)_{n-1}(\lambda^\pm-\lambda^\mp+1)_{n-1}(\lambda_2^\pm+iq/2)_{n-1}(\lambda_2^\pm-iq/2)_{n-1}}, \tag{4.4}$$

with

$$d_a^b = -\frac{1}{2} + a\,\frac{1}{2}\,\sqrt{5-q^2+2b\sqrt{4-3q^2}}, \quad a,b=\pm. \tag{4.5}$$

It is possible to rewrite our ansatz, Eq. (4.3), in terms of the generalized hypergeometric functions

$$f_\omega(x^2) = f_0 + A_1^+ \frac{1}{x^2+(\lambda^+)^2}\; {}_9F_8\left({\lambda_2^+,\lambda_4^++iq/2,\lambda_4^+-iq/2,\lambda^+-d_+^+,\lambda^+-d_-^+,\lambda^+-d_+^-,\lambda^+-d_-^-,\lambda^++ix,\lambda^+-ix \atop \lambda^+,2\lambda^++1,\lambda^++\lambda^-+1,\lambda^+-\lambda^-+1,\lambda_2^++iq/2,\lambda_2^+-iq/2,\lambda_2^++ix,\lambda_2^+-ix}\Big| y\right)$$
$$+ A_1^- \frac{1}{x^2+(\lambda^-)^2}\; {}_9F_8(\lambda^+ \leftrightarrow \lambda^- | y). \tag{4.6}$$

The conditions which determine the coefficients f_0, A_1^+, A_1^- are also analogous to the ones used in the case of $q=0$. The condition obtained by taking the limit $x\to\infty$, or $k\to\infty$, has the form

$$-\frac{1}{A_0\epsilon} = f_0\left[\frac{A_0}{q^2+4} + \frac{2\epsilon-1}{\epsilon}\right] + A_1^+\left[\frac{A_0\lambda_3^+}{\lambda^+(q^2+4)[(\lambda_2^+)^2+q^2/4]}\; {}_7F_6\left({\lambda_4^+,\lambda_4^++iq/2,\lambda_4^+-iq/2,\lambda^+-d_+^+,\lambda^+-d_-^+,\lambda^+-d_+^-,\lambda^+-d_-^- \atop \lambda_3^+,2\lambda^++1,\lambda^++\lambda^-+1,\lambda^+-\lambda^-+1,\lambda_3^++iq/2,\lambda_3^+-iq/2}\Big| y\right)\right.$$
$$\left. + \frac{2\lambda_2^+}{\lambda^+[(\lambda_2^+)^2+q^2/4]}\; {}_7F_6\left({\lambda_3^+,\lambda_4^++iq/2,\lambda_4^+-iq/2,\lambda^+-d_+^+,\lambda^+-d_-^+,\lambda^+-d_+^-,\lambda^+-d_-^- \atop \lambda_2^+,2\lambda^++1,\lambda^++\lambda^-+1,\lambda^+-\lambda^-+1,\lambda_3^++iq/2,\lambda_3^+-iq/2}\Big| y\right)\right] + A_1^-[\lambda^+ \leftrightarrow \lambda^-]. \tag{4.7}$$

We have found that it is convenient to use as the last two conditions the absence of normal thresholds (see discussion at the end of Sec. III B):

$$f_\omega\left(\left(\frac{q}{2}\pm 2i\right)^2\right)=2\,f_\omega\left(\left(\frac{q}{2}\pm i\right)^2\right). \tag{4.8}$$

The condition corresponding to the lower signs is

$$f_0=A_1^+\left[\frac{1}{[(\lambda^+)^2-(2+iq/2)^2]}\;{}_8F_7\left({\lambda_2^+,\lambda_3^++iq/2,\lambda_4^+-iq/2,\lambda^+-2-iq/2,\lambda^+-d_+^+,\lambda^+-d_-^+,\lambda^+-d_+^-,\lambda^+-d_-^- \atop \lambda^+,2\lambda^++1,\lambda^++\lambda^-+1,\lambda^+-\lambda^-+1,\lambda_2^++iq/2,\lambda_2^+-iq/2,\lambda^+-1-iq/2}\Big|y\right)\right.$$
$$\left.-\frac{2}{[(\lambda^+)^2-(1+iq/2)^2]}\;{}_8F_7\left({\lambda_2^+,\lambda_4^++iq/2,\lambda_4^+-iq/2,\lambda^+-1-iq/2,\lambda^+-d_+^+,\lambda^+-d_-^+,\lambda^+-d_+^-,\lambda^+-d_-^- \atop \lambda^+,2\lambda^++1,\lambda^++\lambda^-+1,\lambda^+-\lambda^-+1,\lambda_3^++iq/2,\lambda_2^+-iq/2,\lambda^+-iq/2}\Big|y\right)\right]+A_1^-[\lambda^+\leftrightarrow\lambda^-]. \tag{4.9}$$

The other equation is obtained from the above one by the substitution $q\leftrightarrow -q$.

The difference of these two conditions can be written in the limit $q\to 0$ as

$$A_1^+\left\{\frac{1}{-iq}+O(1)\right\}+A_1^-\{-iCq+O(q^2)\}=0. \tag{4.10}$$

Therefore

$$A_1^+=A_1^-[Cq^2+O(q^3)], \tag{4.11}$$

where C is some constant.

We see that at $q\to 0$ the series of poles $\sim A_n^+/[x^2+(\lambda_n^+)^2]$ decouples from the solution in accordance with our previous considerations for $q=0$.

In this way we have solved Eq. (2.11) for arbitrary momentum transfer q. The solution f_ω is given by Eq. (4.6) with the coefficients f_0, A_1^+, and A_1^- determined from linear system of equations (4.7), (4.8), (4.9).

B. Properties of the partial wave

We investigate the partial wave $F_\omega(q^2)$ obtained from the solution by Eq. (2.9):

$$F_\omega(q^2)=\frac{\epsilon A_0}{q^2+4}\left[f_0+\frac{A_1^+\lambda_3^+}{\lambda^+[(\lambda_2^+)^2+q^2/4]}\;{}_7F_6\left({\lambda_4^+,\lambda_4^++iq/2,\lambda_4^+-iq/2,\lambda^+-d_+^+,\lambda^+-d_-^+,\lambda^+-d_+^-,\lambda^+-d_-^- \atop \lambda_3^+,\lambda_3^++iq/2,\lambda_3^+-iq/2,2\lambda^++1,\lambda^++\lambda^-+1,\lambda^+-\lambda^-+1}\Big|y\right)\right.$$
$$\left.+\frac{A_1^-\lambda_3^-}{\lambda^-[(\lambda_2^-)^2+q^2/4]}\;{}_7F_6\left({\lambda_4^-,\lambda_4^-+iq/2,\lambda_4^--iq/2,\lambda^--d_+^+,\lambda^--d_-^+,\lambda^--d_+^-,\lambda^--d_-^- \atop \lambda_3^-,\lambda_3^-+iq/2,\lambda_3^--iq/2,2\lambda^-+1,\lambda^++\lambda^-+1,\lambda^--\lambda^++1}\Big|y\right)\right]. \tag{4.12}$$

First of all it should be noted that all equations above are written under the assumption that we choose the convention for the square root expression for $\lambda^\pm$ with the real parts of $\lambda^\pm$ being positive for small q and real $\epsilon>-\frac{1}{2}$.

If $q^2\geqslant\frac{9}{10}$, $\lambda^\pm$ are complex conjugate numbers if ϵ belongs to the interval $[\epsilon_1,\infty]$, where $\epsilon_1=(13q^2-3q\sqrt{q^2+16})/2(9-10q^2)$. Since $-1/2<\lambda_1<0$, for any positive ω and therefore for any positive ϵ, $\lambda^\pm$ are complex conjugate. Let us choose by the definition of λ^+ the expression which has a negative imaginary part (for $q>0$).

In the following we study the Regge singularities and the behavior at $-q^2=t\to-\infty$ and at positive t up to the first threshold $t=4$.

Since the solution behaves smooth at $q\to 0$, we conclude that at small q the structure of the Regge singularities is similar to what we have found for $q=0$. The position of the leading Regge pole depends on $t=-q^2$. The result of the numerical calculations is plotted in Fig. 2 for values of t from -4 up to the vicinity of the first threshold at $t=4$. The trajectory is almost linear in the vicinity of $t=0$ with the approximate slope $0.34\alpha_S/m^2$ as shown in Fig. 3.

We would like to mention that the Pomeron trajectory has about the same slope $[\alpha_P'(0)]$ as the gluon trajectory. More interesting would be, within the same approach, to compare the Pomeron trajectory with the Reggeon trajectory. In order to do so one has to calculate the Reggeon trajectory in 2 + 1 QCD using the techniques developed in Ref. [21]. It will be a challenging problem for the future.

At larger $|t|$ the trajectory deviates strongly from the linear behavior. It goes to infinity for t approaching the threshold $t=4$ and returns from $-\infty$ above the threshold. The behavior of the Pomeron trajectory near $t=4$ has been obtained also by solving Eq. (2.13) in the asymptotics of large ω and $t\to 4$ with the result

$$\omega_0(t)|_{t\to 4}=\frac{g^2}{2\pi m}\,\frac{A_0}{4-t}. \tag{4.13}$$

This confirms the numerical result of Fig. 2.

The branch points $\omega_1=0$, $\omega_2=-g^2/\pi m$ do not depend on t. However, the singularities located at the unphysical

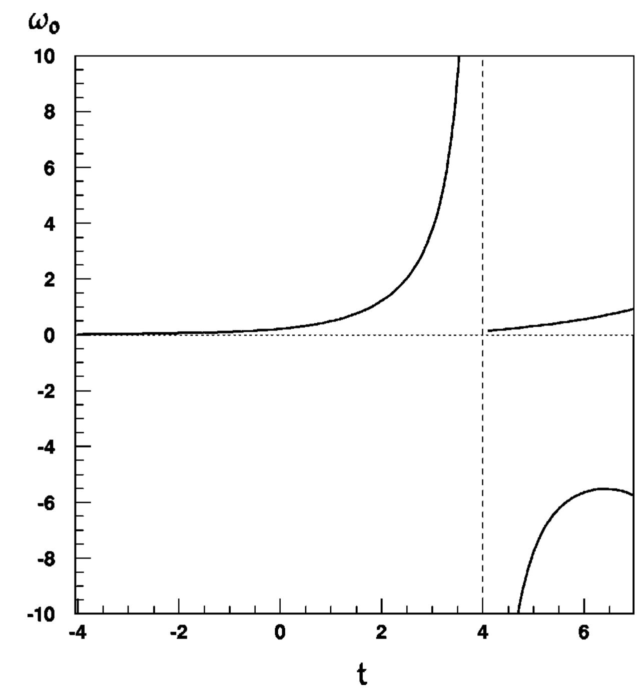

FIG. 2. The trajectory of the Pomeron pole in units of $g^2/2\pi m$. The momentum transfer is given in units of m^2.

sheet can come up to the physical sheet as t increases. Indeed both the poles arising from the lower coefficients β_i in the hypergeometric functions and the poles at the vanishing determinant depend on q. There are also branch points arising from the square roots in the expressions of $\lambda^{\pm}$ in terms of ω, Eq. (4.2), the position of which depend on q. The numerical investigation of the solution shows that besides of the pole,

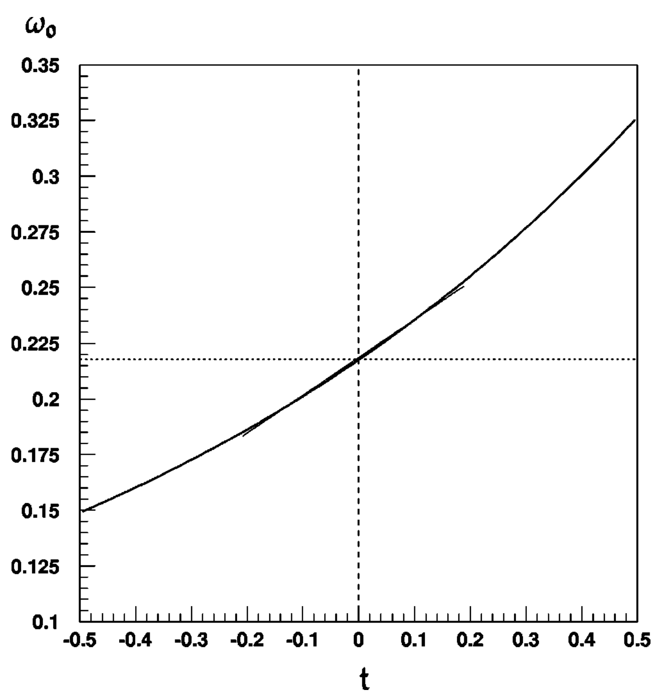

FIG. 3. The behavior of the Pomeron trajectory in the vicinity of $t=0$.

which was originally the leading one, another pole emerges from the unphysical sheet if t crosses the threshold value.

Now we investigate the behavior at $t\to-\infty$. In the limit of large q we have

$$\lambda^{\pm}=k\mp\frac{iq}{2}+O\left(\frac{1}{q}\right),\quad k=\sqrt{\frac{4+5\epsilon}{1+2\epsilon}},$$

and

$$d_a^b=a\frac{iq}{2}+\tau^{(a\cdot b)},\quad \tau^{(a)}=\frac{a\sqrt{3}-1}{2}.$$

Inserting these relations into the linear system we have found that, asymptotically in q,

$$f_0=-\frac{1}{2q^2},$$

$$A_1^+=-A_1^-,$$

$$A_1^+=iqf_0\left\{\frac{2f_2}{k+1}+\frac{2f_4}{k-1}-\frac{f_1}{k+2}-\frac{f_3}{k-2}\right\}^{-1},$$

where

$$f_1={}_3F_2\left({k+\tau^{(+)},k+\tau^{(-)},k+2 \atop 2k+1,k+1}\Big|y\right),$$

$$f_2={}_3F_2\left({k+\tau^{(+)},k+\tau^{(-)},k+3 \atop 2k+1,k+2}\Big|y\right),$$

$$f_3={}_4F_3\left({k+\tau^{(+)},k+\tau^{(-)},k+3,k-2 \atop 2k+1,k+1,k-1}\Big|y\right),$$

$$f_4={}_4F_3\left({k+\tau^{(+)},k+\tau^{(-)},k+3,k-1 \atop 2k+1,k+1,k}\Big|y\right).$$

As a result we obtain from Eq. (4.12) the asymptotics of the partial wave:

$$F_\omega(q^2)|_{q^2\to\infty}\to\frac{\epsilon}{q^2}\left\{1-\frac{2f_2}{k+1}\Big/\left(\frac{2f_2}{k+1}+\frac{2f_4}{k-1}-\frac{f_1}{k+2}-\frac{f_3}{k-2}\right)\right\}.$$

The behavior of F_ω near the right branch point $\omega=0$ is $F_\omega|_{q^2\to\infty}\sim\text{const}/\omega$. This is to be compared with the behavior at the same point for $q=0$, $F_\omega|_{q^2=0}\sim\text{const}$. The numerical calculation of the Pomeron trajectory (see Fig. 2) shows that the pole is moving towards the right branch point with decreasing t. From both observations we conclude that the Pomeron pole moving with t reaches the right branch point $\omega=0$ asymptotically for $t=-q^2\to-\infty$.

V. COMPARISON WITH THE MASSLESS CASE

Li and Tan [14] investigated $(2+1)$-dimensional QCD without symmetry breaking, i.e., for massless gluons, and obtained just a fixed cut starting at $j=1$ as the leading singularity in the vacuum exchange channel. We try to understand the relation of their result to ours, in particular whether the Pomeron pole is absent in the massless case and how it disappears at $m \to 0$.

The infrared singularities in $2+1$ dimensions are stronger compared to $3+1$ dimensions. The limit $m \to 0$ has to be performed carefully. Clearly, the scattering amplitude of vector bosons has no finite limit at $m \to 0$. We consider the scattering of two color dipoles of transverse sizes x_1, x_2, which is the case studied in [14]. The partial wave of the dipole-dipole forward scattering is given by the convolution of two dipole impact factors [14] (here x_0 is the size of the dipole)

$$\Phi_D(x,k) = A \sin^2 kx_0, \tag{5.1}$$

with the Reggeon Green function

$$F^D_\omega(x_{10}, x_{20}) = \int \frac{dk_1 dk_2}{(2\pi)^2} \frac{\Phi_D(x_{10},k_1)}{k_1^2+m^2} \times G_\omega(k_1,k_2) \frac{\Phi_D(x_{20},k_2)}{k_2^2+m^2}. \tag{5.2}$$

The Reggeon Green function is the particular solution of the BFKL equation with δ functions as inhomogeneous term. It is related to our solution $f_\omega(k)$ which is more closely related to the vector boson scattering as follows:

$$\frac{A_0}{\omega(k^2+m^2)} f_\omega(k) = \int_{-\infty}^{\infty} G_\omega(k,k_1) \frac{dk_1}{k_1^2+m^2}. \tag{5.3}$$

Near the Pomeron pole we have

$$G_\omega(k_1,k_2) \approx \frac{\psi_0(k_1)\psi_0(k_2)}{\omega-\omega_0}, \quad \omega_0 = \frac{g^2}{m}\frac{1}{2\pi\epsilon_0}, \tag{5.4}$$

where $\psi_0(k)$ is the wave function of the two-boson bound state corresponding to the Pomeron. It is normalized to 1 and can be obtained from f_ω by studying Eq. (5.3) near ω_0. ϵ_0 is the number quoted in Eq. (3.32).

Restoring the mass dependence we obtain, from the solution (3.21),

$$f_\omega(k) = \frac{1}{m^2}\phi\left(\frac{g^2}{m}\frac{1}{2\pi\omega}, \frac{k}{m}\right). \tag{5.5}$$

The solution depends smoothly on k and the integral with a bounded function $\Phi_D(x,k)$ exists. Therefore also $\psi_0(k)$ has these features

$$\psi_0(k) = \frac{a}{\sqrt{m}} \tilde{\phi}\left(\frac{k}{m}\right), \tag{5.6}$$

with a being some numerical constant. The contribution of the Pomeron pole to the scattering of two colorless dipoles with sizes x_{10} and x_{20} is given at small m by the partial wave

$$F^D_\omega \approx \frac{bg^4}{\omega - \frac{g^2}{m}\frac{1}{2\pi\epsilon_0}} m x_{10}^2 x_{20}^2. \tag{5.7}$$

Here b is some number. This leading contribution to the forward scattering of dipoles does not behave smoothly at $m \to 0$. The pole goes to plus infinity, resulting in a divergent contribution. Expanding in g^2 we observe that the divergence starts at the g^4 term, corresponding to an s-channel intermediate state with two additional gluons.

This observation is confirmed by calculating $G_\omega(k_1,k_2)$ iteratively and evaluating the corresponding contribution to the dipole scattering partial wave, Eq. (5.2), in the following way. We have to iterate Eq. (2.13) with the inhomogeneous term replaced by $\delta(k_1-k_2)$, which is the zeroth approximation of G_ω. Unlike above in Secs. III B and IV A the iteration now proceeds order by order in g^2 or ϵ. Replacing G_ω in Eq. (5.2) by $\delta(k_1-k_2)$ we obtain that the region of $k_1, k_2 \sim m$ gives a negligible contribution for $m \to 0$. Taking the first order approximation in ϵ for G_ω leads to a finite contribution of that small-k region. With the $\mathcal{O}(\epsilon^2)$ approximation for G_ω we obtain a contribution divergent like $1/m$. Starting from this order of perturbative expansion the amplitude of forward dipole-dipole scattering does not exist in the massless limit.

Consider now the scattering at nonvanishing momentum transfer. Let us fix the value t_{phys} in physical units (GeV^2) and look at the relation to our dimensionless variable $t = -q^2$ (in units of m^2):

$$t_{phys} = tm^2. \tag{5.8}$$

Provided $t_{phys} < 0$, the corresponding value of t approaches $-\infty$ at $m \to 0$. Thus the Pomeron pole approaches the branch point at $j=1$.

The singular contribution (5.7) appearing only at $t_{phys} = 0$ is absent in the infrared finite dipole scattering amplitude constructed in [14].

Let us now study the massless limit directly in the equation. We restore the masses in Eq. (2.13) and do the shift $k \to k - q/2$ as in Eq. (4.1):

$$\left[1+\epsilon\left(\frac{(k-q/2)^2+m^2}{(k-q/2)^2+4m^2}+\frac{(k+q/2)^2+m^2}{(k+q/2)^2+4m^2}\right)\right] f_\omega(k,q) = A_0^{-1} + \epsilon m \int \frac{dk_1}{2\pi}\left(\frac{A_0}{[(k_1+q/2)^2+m^2][(k_1-q/2)^2+m^2]} + \frac{2}{(k-k_1)^2+m^2}\left[\frac{(k+q/2)^2+m^2}{(k_1+q/2)^2+m^2}+\frac{(k-q/2)^2+m^2}{(k_1-q/2)^2+m^2}\right]\right) \times f_\omega(k_1,q). \tag{5.9}$$

We perform the Fourier transformation with respect to k,

$$f_\omega(x,q)=\int \frac{dk}{2\pi}e^{-ikx}f_\omega(k,q), \tag{5.10}$$

and obtain

$$\begin{aligned}(1+2\epsilon-2\epsilon e^{-m|x|})f_\omega(x,q)-\frac{3}{2}\epsilon m\int dy\, f_\omega(y,q)\cos\frac{q}{2}(y-x)e^{-2m|x-y|}\\ =\frac{1}{A_0}\delta(x)+\epsilon\delta(x)\left(\frac{A_0}{q^2+4m^2}+2\right)\int dy\, f_\omega(y,q)e^{-m|y|}\cos\frac{q}{2}y+\frac{2A_0\epsilon m\,\delta(x)}{q(q^2+4m^2)}\int dy\, f_\omega(y,q)e^{-m|y|}\sin\frac{q}{2}|y|\\ -\epsilon m e^{-m|x|}\int dy\, f_\omega(y,q)\cos\frac{q}{2}(y-x)e^{-m|x-y|}[2\,\mathrm{sgn}(x)\mathrm{sgn}(x-y)+1].\end{aligned} \tag{5.11}$$

It should be stressed that Eq. (5.11) is the general BFKL equation for $2+1$ QCD in coordinate space at any value of the momentum transfer $t=-q^2$.

As discussed above the behavior at $m=0$ is different for forward and nonforward cases. Indeed the coefficient of second term on the right-hand side (RHS) $\epsilon(A_0/(q^2+4m^2)+2)$, vanishes at $m\to 0$ for $q\neq 0$ but behaves like $1/m$ if we put $q=0$ before taking the limit $m\to 0$. We discuss in the following the massless limit in the nonforward case. We approximate Eq. (5.11) at $m\to 0$, expanding in particular $e^{-m|x|}$, keeping terms ϵm (because $\epsilon=g^2/2\pi m$). In this way we obtain

$$\begin{aligned}(1+2\epsilon m|x|)f_\omega(x,q)-\frac{1}{2}\epsilon m\int dy\, f_\omega(y,q)\cos\frac{q}{2}(x-y)\\ =\frac{1}{A_0}\delta(x)-4\,\delta(x)\frac{\epsilon m}{q}\int dy\, f_\omega(y,q)\sin\frac{q}{2}|y|\\ -2\epsilon m\ \mathrm{sgn}(x)\int dy\, f_\omega(y,q)\cos\frac{q}{2}(x-y)\mathrm{sgn}(x-y).\end{aligned} \tag{5.12}$$

In terms of the function $\tilde{f}_\omega(x,q)$ defined as

$$f_\omega(x,q)=-\left(\frac{d^2}{dx^2}+\frac{q^2}{4}\right)\tilde{f}_\omega(x,q), \tag{5.13}$$

Eq. (5.12) has the following simple form:

$$\left(\frac{d^2}{dx^2}+\frac{q^2}{4}\right)[(1+2\epsilon m|x|)\tilde{f}_\omega(x,q)]=-\frac{\delta(x)}{A_0}. \tag{5.14}$$

The solution has the form

$$(1+2\epsilon m|x|)\tilde{f}_\omega(x,q)=-\frac{1}{qA_0}\sin\frac{q}{2}|x| +A\sin\frac{q}{2}x+B\cos\frac{q}{2}x, \tag{5.15}$$

where A,B are some arbitrary constants.

The original function $f_\omega(x,q)$ can be calculated readily. We write here only part of the result with $A=B=0$, which corresponds to certain boundary conditions:

$$f_\omega(x,q)=\frac{1}{A_0}\left[\frac{\delta(x)}{1+2\epsilon m|x|}-\frac{2\epsilon m\ \cos(q/2)|x|}{(1+2\epsilon m|x|)^2}+\frac{8(\epsilon m)^2\sin(q/2)|x|}{q(1+2\epsilon m|x|)^3}\right]. \tag{5.16}$$

This result has similarities to the expression for the dipole density $n_\omega(x_0,x,q)$ derived by Li and Tan [Eq. (3.4) in the second paper of Ref. [14]]. Our $f_\omega(x,q)$ is not the dipole density and our equation does not know about the dipole size on which $n_\omega(x_0,x,q)$ depends essentially. However, introducing the dipole size $x_0>0$ by replacing the RHS of Eq. (5.14) by $-\delta(x_0-|x|)$ and restricting the range in x to $|x|\neq 0$, we obtain

$$\begin{aligned}G_\omega(x,x_0;q)&=\left(\frac{d^2}{dx^2}+\frac{q^2}{4}\right)\frac{1}{[1+2\epsilon m|x|]}\frac{2}{q}\theta(x_0-|x|)\\ &\quad\times\sin\frac{q}{2}(x_0-|x|)\\ &=\frac{\delta(x_0-|x|)}{1+2\epsilon m|x|}+\theta(x_0-|x|)\\ &\quad\times\left[\frac{16(\epsilon m)^2\sin(q/2)(x_0-|x|)}{q(1+2\epsilon m|x|)^3}+\frac{4\epsilon m\ \cos(q/2)(x_0-|x|)}{(1+2\epsilon m|x|)^2}\right].\end{aligned} \tag{5.17}$$

We denote by $G_\omega(x,x_0;q)$ the analogon of $f_\omega(x,q)$, Eq. (5.13), of the modified equation. This particular solution of the modified equation (5.14) reproduces the dipole density $n_\omega(x_0,x,q)$ of Ref. [14] up to terms proportional to $\delta(x)$.

VI. SUMMARY

The reduction of the dimensionality to $2+1$ simplifies the high-energy scattering amplitudes and in particular the BFKL equation. The equation can be solved analytically even in the case with masses introduced by spontaneous symmetry breaking.

In the forward case we have discussed the solution both in coordinate and momentum space. In coordinate space the similarity of the Pomeron pole to a two-gauge-boson bound state has been emphasized, whereas in the momentum representation the iterative structure becomes transparent, which has been used further to solve the equation in the nonforward case.

We obtain the partial wave for the scattering amplitude of vector bosons in an analytic form. This allows us to study the leading and nonleading Regge singularities and their dependence on the momentum transfer both for negative and positive t.

At small momentum transfer we find a leading Regge pole, the Pomeron, with an intercept above $j=1$ and a trajectory approximately linear for small t. Beside this pole there is a branch cut whose right end is located at $j=1$, independent of t. The Pomeron pole approaches the cut for large negative t.

We have compared our result with the one by Li and Tan [14] and have discussed the peculiarities of the massless limit. This limit is different for the forward and nonforward cases. The massless limit of our result for the nonforward amplitude is close to the result found by Li and Tan who used a quite different approach. A modified equation (by introducing the dipole size as an additional parameter) reproduces the result of these authors. However, in the forward case the Pomeron pole leads to a divergent contribution, which is absent in the amplitude of Ref. [14].

Although the model resides in unphysical $2+1$ dimensions, some features can be related to the phenomenology of high-energy scattering. The leading Pomeron pole which is clearly separated from nonleading singularities corresponds to the common idea about the soft (nonperturbative) Pomeron. Furthermore, a situation with a pole with an intercept larger than 1 and a fixed cut just at 1 would result in a change of the s dependence with t. It is interesting to note that the constant term in the high-energy asymptotics, which corresponds to the cut contribution, has been used to describe the experimental data on the high-energy behavior of total cross sections [17], inclusive spectra [18], and diffractive dissociation [19].

The divergence of the trajectory at $t\to 4m^2$ seems to exhibit an infinite series of bound states of two massive gluons. This would differ clearly from the features of the hadronic reality. We understand that this is an artifact of the leading $\ln s$ approximation, since a potential of finite range created by massive boson exchange cannot have an infinity of bound states.

The simplicity of the model makes it useful for further investigations. Including fermions the amplitudes with quantum number exchange could be constructed. There will be no direct analogy either to the Dokshitzer-Gribov-Lipatov-Altarelli-Parisi (DGLAP) [20] equation or to the nonlinear double-logarithmic equation [21]. More interesting could be the study of amplitudes with multiple exchange of Reggeized gluons, in particular with the exchange of negative charge parity (odderon).

The model can serve as a testing ground for the nonperturbative treatment of diffractive processes [22,23], and the high-parton-density effective action [24]. Also, the effective action of high-energy scattering [25] and Gribov's Reggeon field theory [9] can be studied in the simpler situation of $2+1$ dimensions.

ACKNOWLEDGMENTS

E.M.L., L.N.L., and M.W. want to thank the Aspen Physics Center for the hospitality and creating the working atmosphere during the workshop on ''Interface of ''soft'' and ''hard'' interactions'' where this paper has been started. We are also very grateful to C-I. Tan who drew our attention to the problem of the mismatch between massive and massless $2+1$ dimensional QCD. Without his questions and his strong encouragement this paper would not have been started at all. E.M.L. thanks the theory groups at Fermilab, ANL and DESY where he continued to work on this paper for hospitality and support. D.Yu.I. and L.Sz. would like to acknowledge the warm hospitality extended to them at University of Leipzig. This work was supported by German Bundesministerium für Bildung, Wissenschaft, Forschung und Technologie, Grant No. 05 7LP91 P0, and by the Volkswagen Stiftung.

[1] ZEUS Collaboration, J. Breitweg *et al.*, Phys. Lett. B **407**, 432 (1997); M. Derrick *et al.*, Z. Phys. C **69**, 607 (1996); **72**, 394 (1996); H1 Collaboration, S. Aid *et al.*, Nucl. Phys. **B470**, 3 (1996); **B497**, 3 (1997).
[2] CDF Collaboration, F. Abe *et al.*, Phys. Rev. D **50**, 5535 (1994); Phys. Rev. Lett. **79**, 2636 (1997).
[3] V. S. Fadin, E. A. Kuraev, and L. N. Lipatov, Phys. Lett. **60B**, 50 (1975); Sov. Phys. JETP **44**, 443 (1976); **45**, 199 (1977); Y. Y. Balitski and L. N. Lipatov, Sov. J. Nucl. Phys. **28**, 822 (1978).
[4] A. Donnachie and P. V. Landshoff, Nucl. Phys. **B244**, 322 (1984), **B267**, 690 (1986); Phys. Lett. B **296**, 227 (1992); Z. Phys. C **61**, 139 (1994).
[5] E. Gotsman, E. Levin, and U. Maor, Phys. Lett. B **309**, 199 (1993); Phys. Rev. D **49**, R4321 (1994).
[6] E. Levin, ''Everything about Reggeons. Part 1: Reggeons in

''soft'' interactions,'' Report No. TAUP 2465-97, DESY 97-213, hep-ph/9710546.
[7] R. Feynman, *Photon-hadron Interaction* (Benjamin, New York, 1972).
[8] V. N. Gribov, ''Space-time description of hadron interactions at high energies,'' (in Russian), 1973, In Moscow 1 ITEP School, Vol. 1 ''Elementary particles'' (Energoatomizdat, Moscow, 1973), p. 65.
[9] V. N. Gribov, Sov. Phys. JETP **26**, 414 (1968).
[10] A. R. White, Phys. Rev. D (to be published), hep-ph/9712466, and references therein.
[11] R. K. Ellis, W. J. Stirling, and B. R. Webber, *QCD and Collider Physics* (Cambridge University Press, Cambridge, UK, 1996), p. 435; A. M. Cooper-Sarkar, R. C. E. Devenish, and A. De Roeck, ''Structure functions of the nucleon and their interpretation,'' Report No. OUNP-97-10, DESY 97-226 and references therein.
[12] L. N. Lipatov and L. Szymanowski, ''Some remarks on the Pomeranchuck singularity in non-abelian gauge theories,'' Institute for Nuclear Research, Warsaw, Report No. 11/VII/80.
[13] L. N. Lipatov, Sov. Phys. JETP **63**, 904 (1986).
[14] Miao Li and Chung-I Tan, Phys. Rev. D **50**, 1140 (1994); **51**, 3287 (1995).
[15] G. M. Cicuta, G. Marchesini, and E. Montaldi, Phys. Lett. **96B**, 141 (1980).
[16] A. P. Prudnikov, Yu. A. Brychkov, and O. I. Marichev, *Integrals and Series* (Gordon and Breach, New York, 1990), Vol. 3.
[17] B. Z. Kopeliovich, I. K. Potashnikova, and N. N. Nikolaev, Phys. Lett. B **209**, 355 (1988); E. Gotsman, E. M. Levin, and U. Maor, Z. Phys. C **57**, 667 (1993).
[18] A. K. Likhoded, V. A. Uvarov, and P. V. Chliapnikov, Phys. Lett. B **215**, 417 (1988).
[19] Chung-I Tan, ''Flavoring of Pomeron and diffractive production at Tevatron energies,'' Report No. BROWN-HEP-1100, hep-ph/9711404, 1997.
[20] L. N. Lipatov, Sov. J. Nucl. Phys. **20**, 94 (1974); G. Altarelli and G. Parisi, Nucl. Phys. **B126**, 298 (1977); Yu. L. Dokshitzer, Sov. Phys. JETP **46**, 641 (1977).
[21] R. Kirschner and L. N. Lipatov, Nucl. Phys. **B213**, 122 (1983).
[22] O. Nachtman, Ann. Phys. (N.Y.) **209**, 436 (1991); ''High Energy Collisions and Nonperturbative QCD,'' in Schladming School 1996, Perturbative and Nonperturbative Aspects of QCD, pp. 49–138, hep-ph/9609365; H. G. Dosch, E. Ferreira, and A. Krámer, Phys. Rev. D **50**, 1992 (1994).
[23] W. Buchmüller and A. Hebecker, Nucl. Phys. **B476**, 203 (1996); W. Buchmüller, M. F. McDermott, and A. Hebecker, *ibid.* **B487**, 283 (1997); W. Buchmüller and A. Hebecker, Phys. Lett. B **B355**, 573 (1995).
[24] L. McLerran and R. Venugopalan, Phys. Rev. D **49**, 2233 (1994); **49**, 3352 (1994); **50**, 2225 (1994); **53**, 458 (1996); J. Jalilian-Marian *et al.*, *ibid.* **55**, 5414 (1997); Nucl. Phys. **B504**, 415 (1997); hep-ph/9706377; hep-ph/9709432.
[25] R. Kirschner, L. N. Lipatov, and L. Szymanowski, Nucl. Phys. **B245**, 579 (1994); Phys. Rev. D **51**, 838 (1995); L. N. Lipatov, Nucl. Phys. **B452**, 369 (1995).